January 16, 2018

Mr. Brandon Forsythe
The Pennsylvania State University
2217 Earth and Engineering Sciences Building
University Park, PA 16802

Subject: Results of Geophysical Borehole Logging
Two Boreholes (CZMW-4 and CZMW-10)
Shale Hills
Petersburg, PA
ARM Project: 170597

Dear Mr. Forsythe,

ARM Geophysics (ARM) is pleased to present this letter report that summarizes the results of geophysical borehole logging performed at the above referenced site on November 21, 2017. The objectives of the logging were to identify water-bearing zones and to measure the depth and orientation of fractures and bedding planes in the above mentioned boreholes. To achieve these objectives, ARM acquired standard borehole logs and images as discussed below.

## LOGGING METHODS

The logs that ARM completed for this investigation include:

- Natural Gamma
- Fluid Temperature
- Fluid Conductivity
- 3-Arm Caliper
- Short & Long Normal Resistivity
- Full Waveform Sonic (FWS)
- Single Point Resistance
- Spontaneous Potential (SP)
- Optical Televiewer (OTV)
- Acoustic Televiewer (ATV)
- Neutron
- Density

ARM has provided a summary of these logging methods in Attachment A. ARM acquired all the logs using a Matrix acquisition system and tools manufactured by Mount Sopris Instrument Company.

## INTERPRETATION

### BASIC LOG DESCRIPTIONS

The geophysical borehole logs acquired during this investigation are presented in Attachment B. All log depths are referenced to ground surface as indicated in the header of each log. The majority of the acquired data are presented as standard curves that represent the change in measured parameter with depth. The format of the heat pulse flowmeter and televiewer logs are discussed in the following paragraphs.

The Vertical Flow track in the Hydro Log provides a record of the rate of vertical fluid movement derived from the heat pulse flowmeter tool. The X-axis represents the magnitude of flow in gallons/min that was recorded at depths indicated by the posted value. It is calculated during acquisition by dividing the distance between the grid and thermistors by the travel time. Negative and positive values indicate downward and upward flow, respectively.

The televiewer logs contain borehole images and structural information obtained from the OTV tool. The *Optical View* track is an "unwrapped" photographic image of the borehole wall (Figure 1). In this case, the cylindrical borehole surface is unzipped along the north azimuth and unrolled to a flat strip. The compass orientation (with respect to true north) is presented at the top of the log. The unwrapped format is distorted like any projection of a curved surface on a flat one. Horizontal and vertical planes will be undistorted. However, dipping planes will be represented as a sine wave: the greater the dip, the greater the wave amplitude.

The Plane Projection track presents the fracture signatures that are digitized from the unwrapped *Optical View* track. The *Dip & Dip Direction* log is a presentation in which the vertical axis is depth and the horizontal is dip angle from 0° to 90°. As shown in Figure 2, the dip direction is indicated by the orientation of the tadpole tail, measured in a clockwise direction from north.

## INTERPRETATION OF STRUCTURAL DIAGRAMS

The structural data are presented on polar and rose diagrams for statistical analysis and pattern visualization. Polar diagrams are used in this report to plot the dip and dip direction of planar features. Zero degree dip is represented at the center of the diagram and 90° at the circumference. The dip direction is indicated by the compass azimuth, measured clockwise from north (0°), as shown in Figure 3. This format is sometimes referred to as a dip vector plot but it is essentially the same as a stereonet with an upper hemisphere projection.

The rose diagram graphically illustrates the strike distribution of a set of planes. Radiating rays are drawn with lengths proportional to number of strike measurements within each 10° sector. It is important to recognize that in this report, the polar diagram represents dip and dip direction, whereas the rose diagram represents strike. Using the right-hand-rule convention, strike equals the dip direction minus 90°.

## FULL WAVEFORM SONIC (FWS)

Sonic logs are typically used to help identify lithology, porosity, and mechanical rock properties. The sonic tool contains acoustic transmitters and receivers. A sound pulse is generated by a transmitter and travels through the formation. One or more receivers record the sound pulse as it passes. The sonic log is simply a record of the time interval at which sound travels through 1 ft of formation. This measurement is called the interval transit time, slowness, or delta t (t) and is the reciprocal of the velocity of the sound wave.

As the sound wave emitted by the transmitter encounters the borehole wall, 1) compressional and shear waves are generated in the formation, 2) surface wave along the borehole wall, and 3) tube waves in the borehole fluid. The first and second sound wave arrivals at the receiver are the compressional (P-wave) and shear (S-wave) arrivals, respectively. These are the most common signals used in sonic logging and their transit times vary with lithology and porosity. In addition, the relationship between the S- and P-waves and density can be used to calculate mechanical rock properties such as Poisson's ratio, bulk modulus, Young's modulus, and shear modulus.

The following parameters were selected for the site based on source to receiver spacing, borehole diameter, and expected compressional wave rock velocities.

- Transmitter frequency, 7 KHz
- Sampling rate, 4 µs
- Holdoff time, 100 µs
- Number of samples, 256

For this project, ARM used a multi-frequency full waveform sonic tool manufactured by Mount Sopris Instruments (Model number 2SAA (F)-1000). The sonic tool was assembled with three receivers, spaced at 3-feet, 4-feet, and 5-feet from the transmitter (see specification sheet in Appendix C). ARM applied a static 3-feet upward depth shift (subtracted 3-feet) to the sonic data to account for the 3-feet separation between the transmitter and the first receiver.

## RESULTS AND DISCUSSION

### ORIENTATION ANALYSIS OF PLANAR FEATURES

The optical and acoustic images were used to measure the depth and orientations of bedding and fracture planes. The digitized planar features were corrected for borehole deviation and magnetic declination. The measured plane projections and orientations are shown in the plane projection logs. A tabulated listing of the bedding and fracture orientations is presented in Attachment C. Stereographic analysis was performed on the planar orientation data acquired from the image logs. A listing of the calculated mean orientations of all bedding and fracture planes are presented in Table 1. The results from the boreholes are presented in the polar and rose diagrams, and charts shown in Figure 4 through 8. Predominant groups or "sets" are indicated by the clustering of data points in the polar diagrams.

Figure 4 presents a polar diagram showing the dip and dip direction of all planes measured during this investigation. ARM has classified the planes by symbols corresponding to bedding and fracture plane sets.

ARM used statistical contouring to identify windows in which to calculate the mean orientation of all bedding and fracture planes. Figure 5 presents a polar diagram with statistical contouring of bedding plane orientations. The mean bedding dip/dip directions are shown to the right of the diagram. The rose diagram in Figure 7 shows a predominant WNW/ESE strike direction.

Figure 6 presents a polar diagram with statistical contouring of all fracture plane orientations. The mean fracture plane dip/dip directions are shown to the right of the diagram. The rose diagram in Figure 8 shows a predominant NE/SW strike direction.

The mean orientations for all bedding planes and fracture sets are shown in Table 1.

Table 1: Statistical mean of dip and dip direction of bedding and fracture planes.

| Planes | Dip | Dip Direction | Strike/Dip |
|---|---|---|---|
| Bedding | 11 | 190 | N80W/11SW |
| Fracture Set | 81 | 144 | N54E/81SE |

## CLOSING

The data collection and interpretation methodologies used in this investigation are consistent with standard practices applied to similar geophysical investigations. The correlation of geophysical responses with probable subsurface features is based on the past results of similar surveys although it is possible that some variation could exist at this site.

Please contact us if you have any questions regarding this survey. We appreciate your business and look forward to working with you again.

Kind regards,
ARM Geophysics

Duro Rajković

Duro Rajkovic
Senior Geophysicist

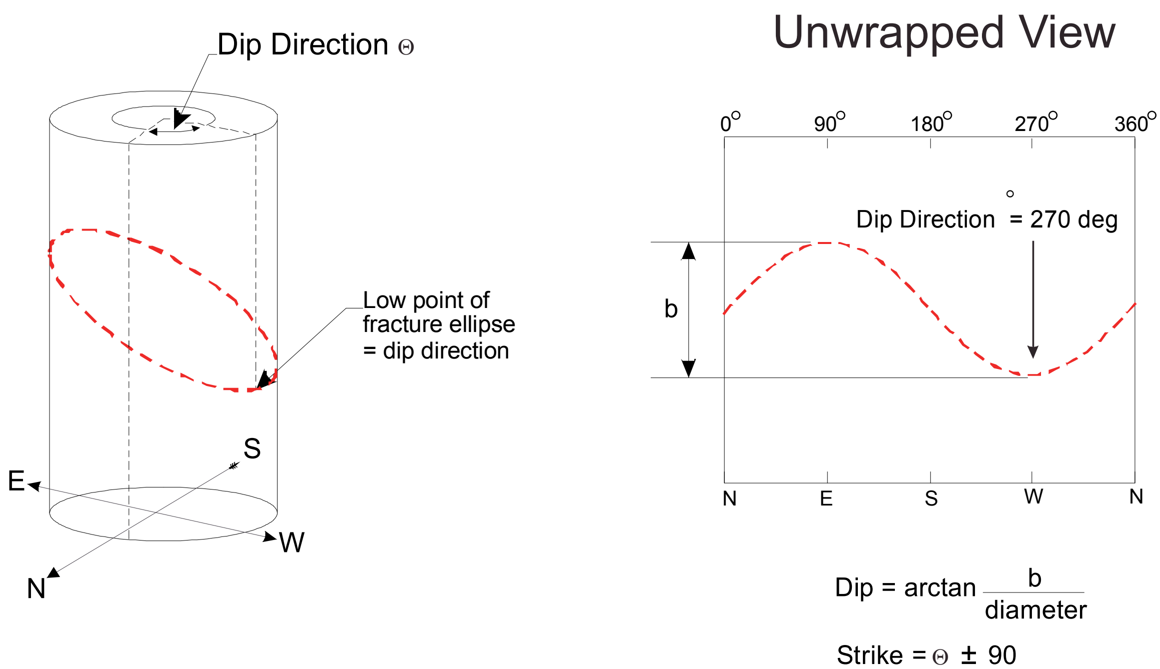


**Figure 1: Diagram illustrating unwrapped view of fracture signature.**

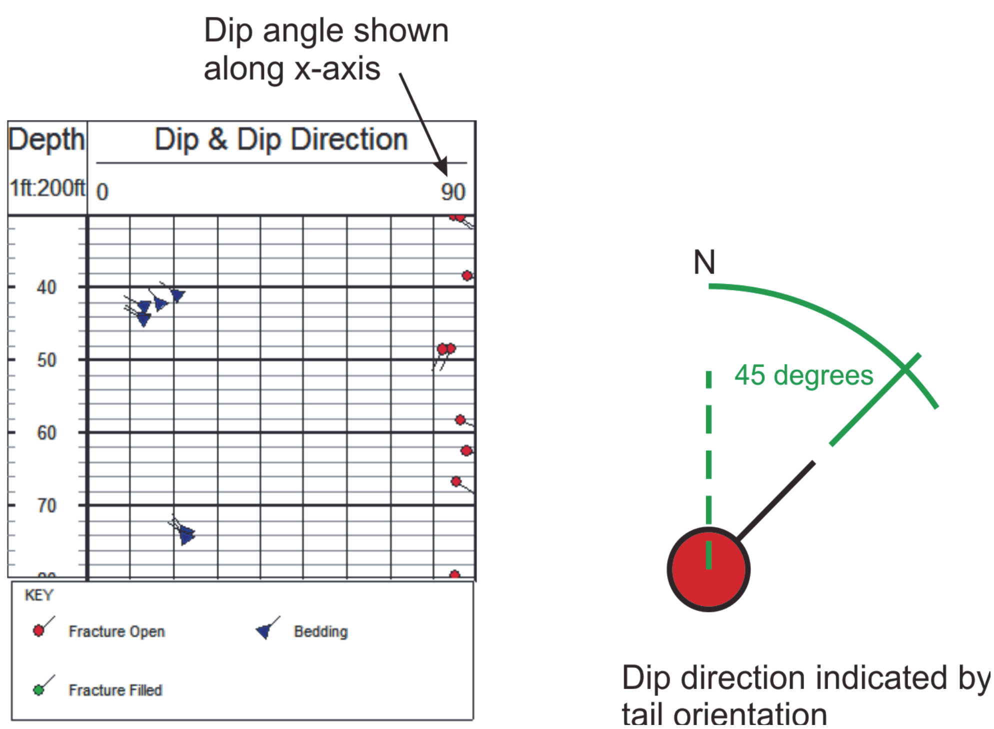


**Figure 2: Dip & dip direction determination from the tadpole plot.**

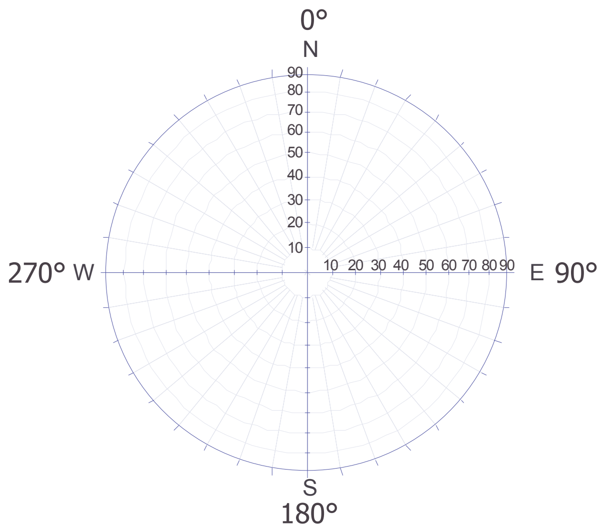


Polar Diagram

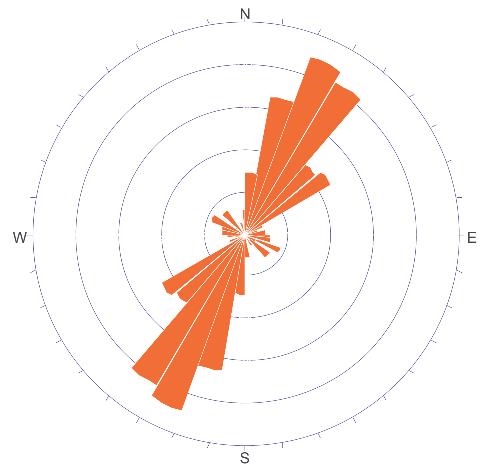


Rose Diagram

**Figure 3: Example polar and rose diagrams. Polar diagram is used in this report for plotting dip and dip direction. Rose diagrams are used for plotting the frequency or number of strike measurements per sector.**

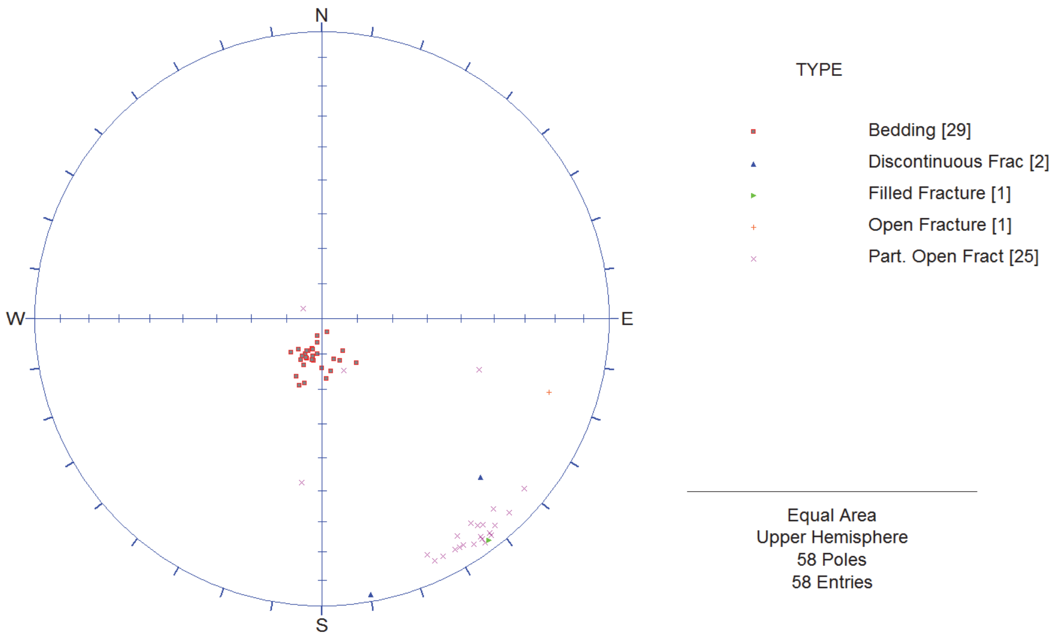


**Figure 4: A polar diagram plotting dip and dip direction of all planes categorized by plane type.**

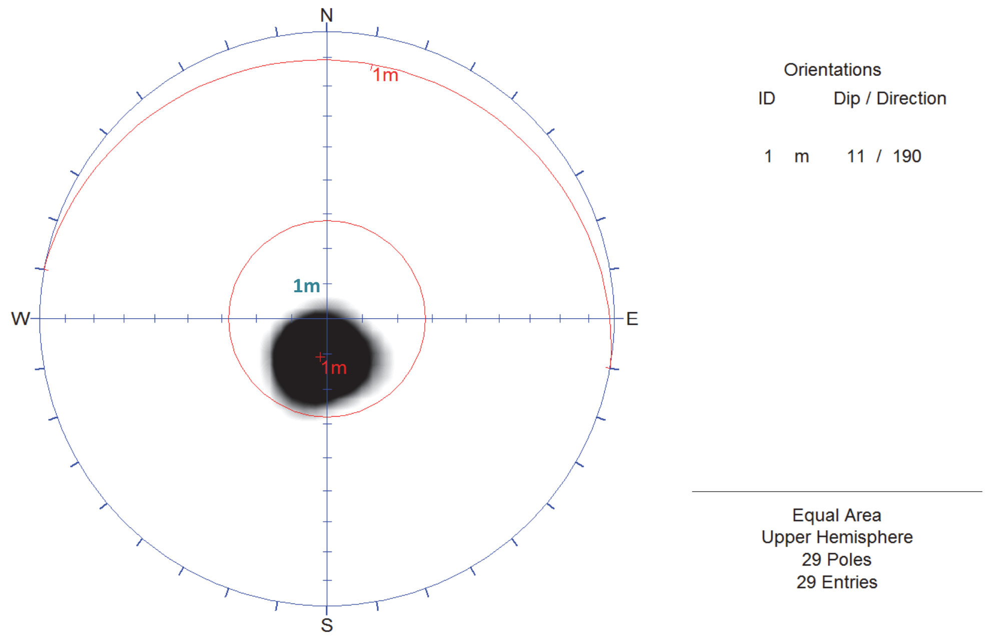


**Figure 5: A polar diagram with statistical contouring of all bedding planes. The calculated mean dip angle and direction is shown at the right of the diagram.**

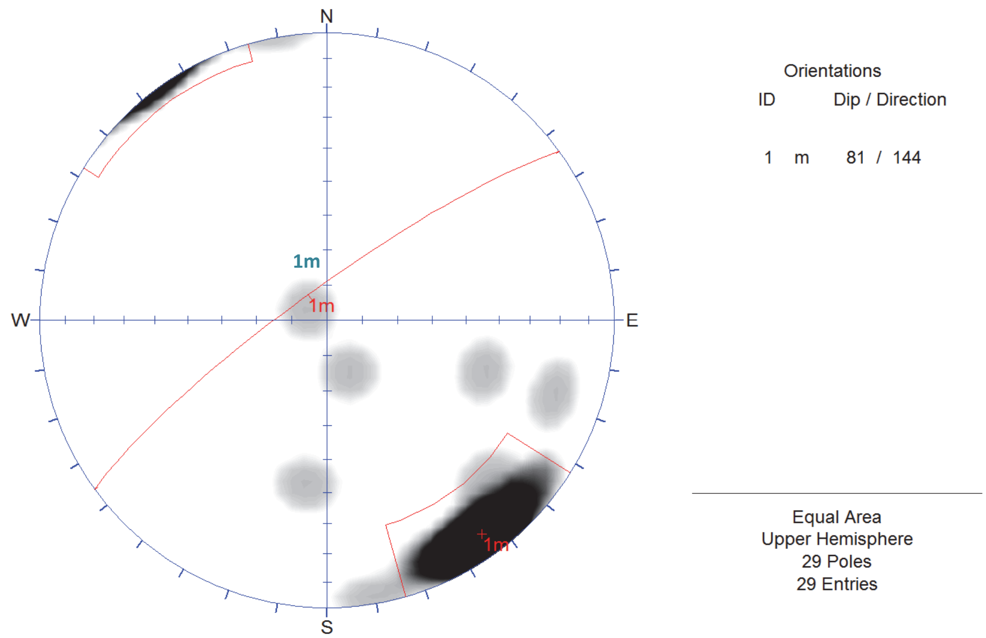


**Figure 6: A polar diagram with statistical contouring of all fracture planes. The calculated mean dip angle and direction is shown at the right of the diagram.**

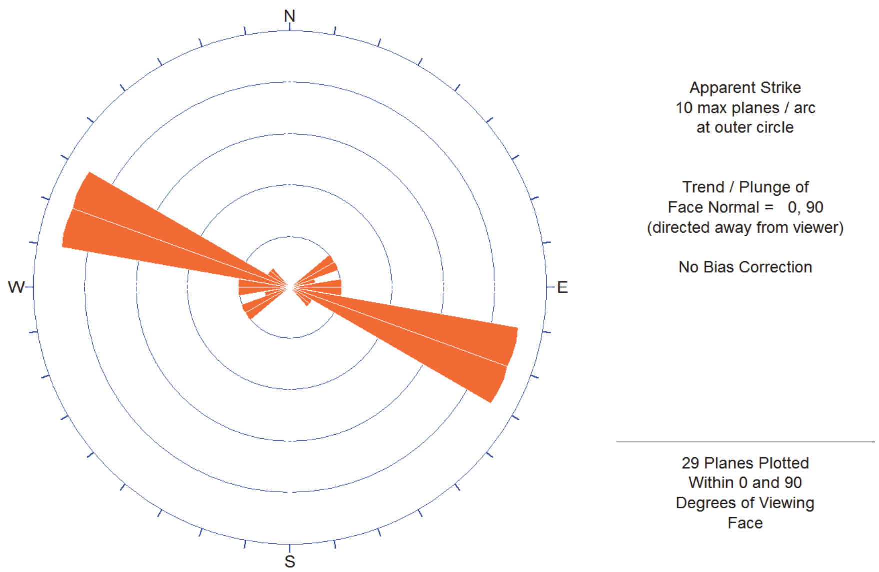


**Figure 7: A rose diagram illustrating strike distribution of all bedding planes.**

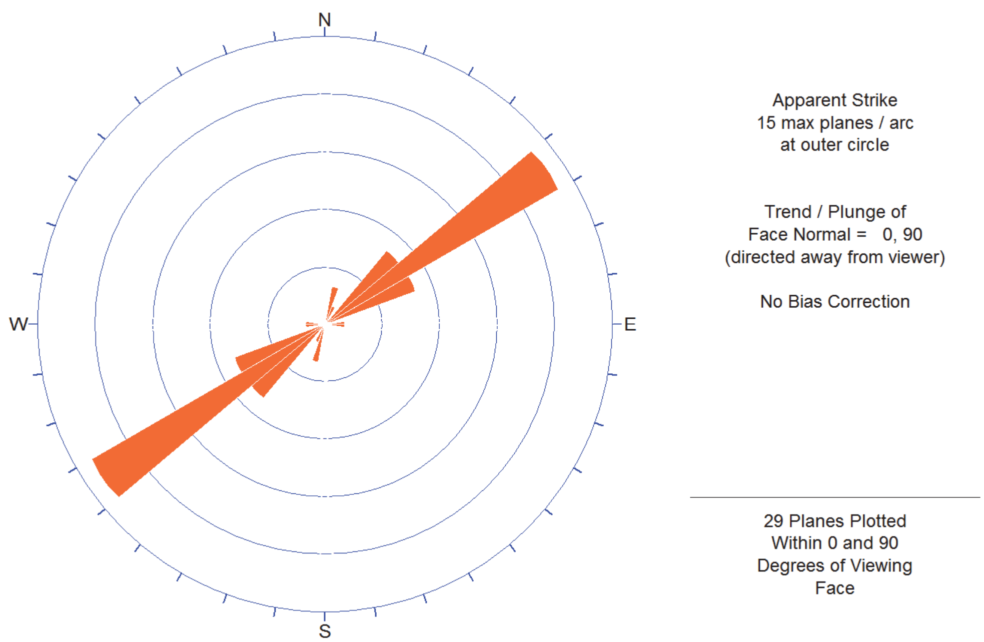


**Figure 8: A rose diagram illustrating strike distribution of all fracture planes.**

# ATTACHMENT A
# LOGGING METHODS

1129 West Governor Road, PO Box 797
Hershey, PA 17033-0797
Voice: (717) 533 - 8600
Fax: (717) 533 - 8605

# APPENDIX A: OVERVIEW OF LOGGING METHODS

## CALIPER LOGS

The caliper log measures variations in borehole size as a function of depth in a well. Some example responses of in a caliper log is shown in Figure A- 1 (Rider, 2002[1.] ) The log data enables (a) the detection of competent or fractured geologic units, (b) the location of washouts or tight zones, (c) the optimal placement of well screen, sand, and bentonite, and (d) the establishment of appropriate borehole correction factors to be applied to other well log curves. Further, when run in combination with other logs, the caliper log may be an indicator of lithologic makeup and degree of consolidation. The typical caliper response in a fractured, weathered, or karstic unit is a relatively abrupt increase in borehole size.

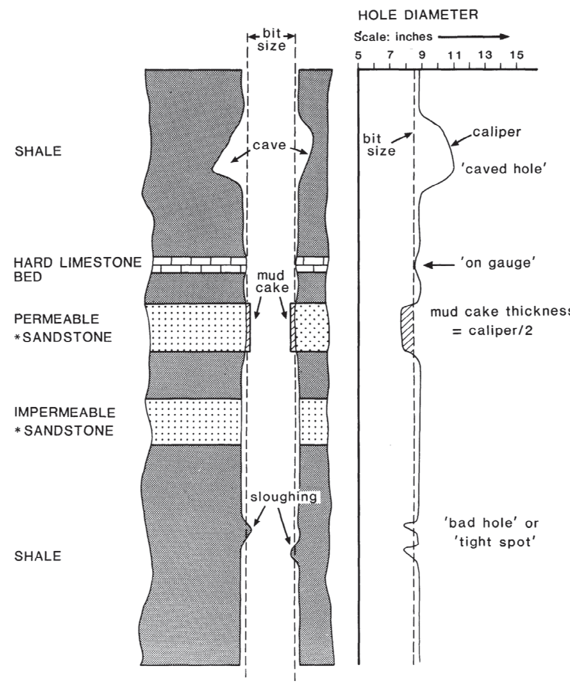


**Figure A- 1: The caliper log showing some typical responses. (From Rider, 2002).**

## SPONTANEOUS POTENTIAL (SP) LOGS

The SP log measures the natural voltages that are created within the borehole due to the presence of borehole fluids, formation fluids, and formation matrix materials. It is recorded by measuring the difference in electrical potential in millivolts between an electrode in the borehole and a grounded electrode at the surface. The SP log is commonly used to 1) detect permeable beds, 2) detect boundaries of permeable beds, 3) determine formation water resistivity, and 4) determine the volume of shale in permeable beds. The constant SP readings observed in thicker shale units define the shale base line, a reference line from which further formation matrix and formation fluid property calculations may be completed. Although this log is consistently used in oil and gas applications, its effectiveness in water wells is limited since the method requires a contrast in salinity between borehole and formation fluids (Figure A- 2). This condition is often not met in ground water wells.

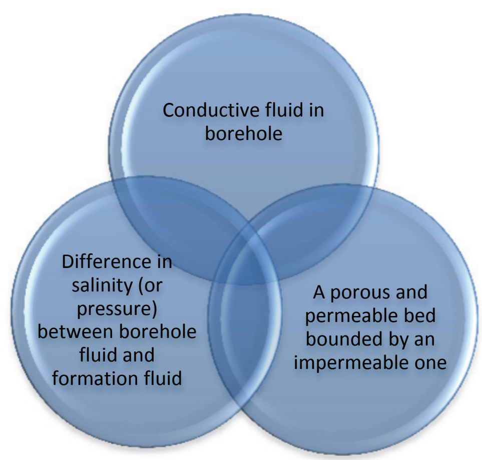


**Figure A- 2: Conditions required to produce an SP response.**

1 Rider, M. (2006) The Geological Interpretation of Well Logs, *Rider-French Consulting, Ltd.*, 280pp.

The SP log can be qualitatively used for permeability recognition. SP deflections from the shale base line commonly indicate the presence of a permeable bed. The magnitude and direction of the deflection is dependent upon the relative resistivity (or salinity) values of the borehole fluid and the formation fluid. If the formation fluid resistivity is less than the borehole fluid resistivity, then the relative SP values will decrease in a porous, coarse-grained unit. Alternately, if the formation fluid resistivity is greater than the borehole fluid resistivity, the relative SP values will increase in the same body, and the curve shape is referred to as a "reversed SP". If both fluid resistivities are equal, no SP deflection will occur.

## GAMMA RAY LOGS

The gamma ray log is a passive instrument that measures the amount of naturally occurring radioactivity from geologic units within the borehole. Commonly occurring radioelements include potassium, thorium, and uranium; the two former elements are predominant within a common fine-grained rock sequence. The gamma ray log is also an excellent lithologic indicator because fine-grained clays and shales contain a higher radioelement concentration than limestones or sands. Gamma ray values are often used to assess the percentage of clay materials (indurated or non-indurated) that are present within a formation by utilizing empirically derived equations and sand-shale base line information.

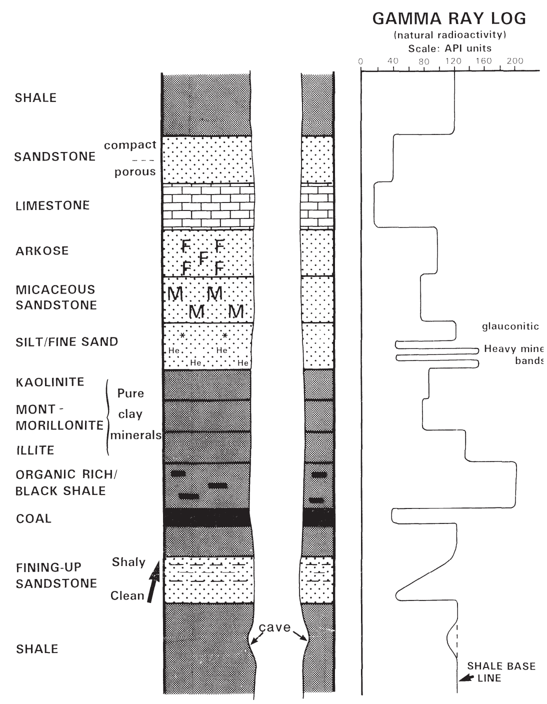


Figure A- 3: Characteristic gamma ray responses. (From Rider, 2002).

## NORMAL RESISTIVITY LOGS

Resistivity is a measure of how well an electric current passes through a material. Formation resistivity is an intrinsic property of rocks and depends on the porosity and resistivity of the interstitial fluid and rock matrix. The spacing between the transmitter and receiver on the tool determines the depth of investigation into the surrounding formation; the greater the spacing, the deeper the penetration of electrical current into the formation.

In sedimentary rocks, the resistivity values of shales (5 - 30 ohm-m) is generally lower than the resistivity of sandstone (30 – 100 ohm-m), which is lower than the resistivity limestone (75 – 300 ohm-m). The resistivity log often shows a picture of the overall depositional sequence in sedimentary environment. Resistivity of igneous and metamorphic rocks is extremely high when compared to resistivity in sedimentary rocks, with values that are commonly thousands of ohm-meters. Example resistivity log responses are shown in Figure A- 4.

## FLUID RESISTIVITY LOGS

Fluid resistivity, which is the reciprocal of fluid conductivity, provides data related to the concentration of dissolved solids in the fluid column. Although the quality of the fluid column may not reflect the quality of adjacent interstitial fluids, information can be quite useful when combined with other logs. For example, change in fluid resistivity associated with a water-producing zone that is corroborated by other logs may indicate the inflow of ground water.

## SINGLE-POINT RESISTANCE LOGS

Single point resistance measurements are made by passing a constant current between two electrodes and recording the voltage fluctuations as the probe is moved up the borehole. The resistance variations measured in the borehole is primarily due to variations in the immediate vicinity of the downhole electrode.

The resistance log is strongly affected by the resistance of the drilling fluid and variations in borehole diameter. It is extremely useful for detecting fractures in boreholes with relatively constant diameter. In sedimentary environments, the resistance log generally follows the variations in resistivity of the formation. Shales in clay generally exhibit low values, sandstones have intermediate values, while coal and limestone beds have high resistance values.

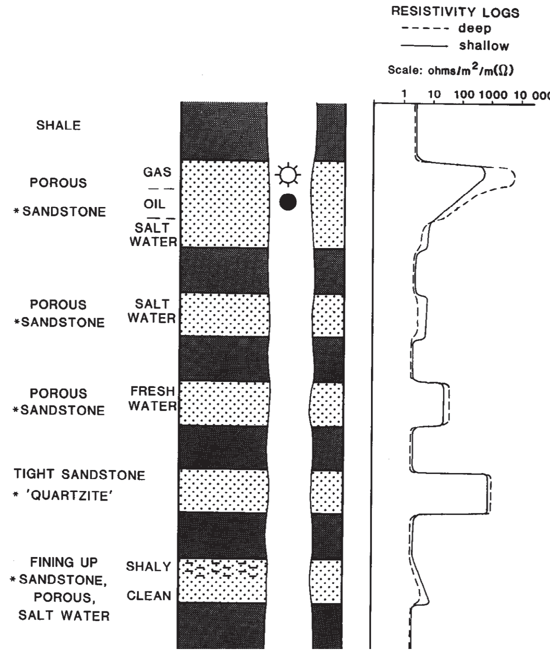


**Figure A- 4: Characteristic resistivity responses. (From Rider, 2002)**

## TEMPERATURE LOGS

Temperature logs measure the change in fluid temperature within the borehole as a function of depth. This log can indicate the location of water- producing strata or fracture zones within the well. The inherent assumption of this technique is that the fluids entering the borehole from water producing zones are either cooler or warmer than the fluid in the borehole. In this case, it is possible to relate a temperature anomaly to a depth range in which waters of different temperature are emanating from a water-producing/receiving or fractured lithologic unit.

## HEAT PULSE FLOWMETER (HPFM) LOGS

The heat pulse flowmeter measures the vertical flow rates within a borehole. The log may be used to identify contributing fracture zones under natural and pumping conditions. The system operates by heating a wire grid that is located between two thermistors. The heated body of water moves toward one of the thermistors under the effect of the vertical component of flow within the well. Positive and negative values on the log represent upward and downward flow, respectively. Measurements are recorded while the tool is stationary and the logs are presented as a bar graph (mud log) as shown in Figure A- 5.

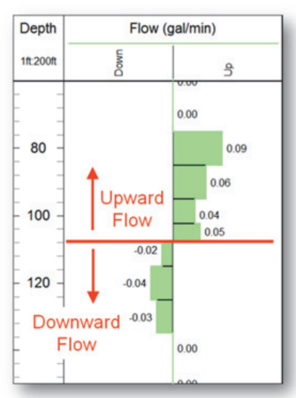


**Figure A- 5: Example heat pulse flowmeter log.**

A number of techniques have been attempted for measuring horizontal flow in wells without much success. The techniques may not represent the true hydrogeologic conditions due to variations in flow caused by the well.

## OPTICAL TELEVIEWER (OTV) LOGS

The optical televiewer probe combines the axial view of a downward looking digital imaging system with a precision ground hyperbolic mirror to obtain an undistorted 360° view of the borehole wall. The probe records one 360° line of pixels at 0.003-ft depth intervals. The sample circle can be divided into 720 or 360 radial samples to give 0.5° or 1° radial resolution. For this investigation, the highest radial resolution (0.5°) was used. The line of pixels is aligned with respect to True North and digitally stacked to construct a complete, undistorted, and oriented image of the borehole walls. The data are 24 -bit true color and may be used for lithologic determination as part of the interpretation. Since the acquired image is digitized and properly oriented with respect to borehole deviation and tool rotation, it allows data processing to provide accurate strike and dip information of structural features. The borehole image is often shown as an "unwrapped" 360° image in which the cylindrical borehole image is sliced down the northern axis and flattened out as shown in Figure A- 6.

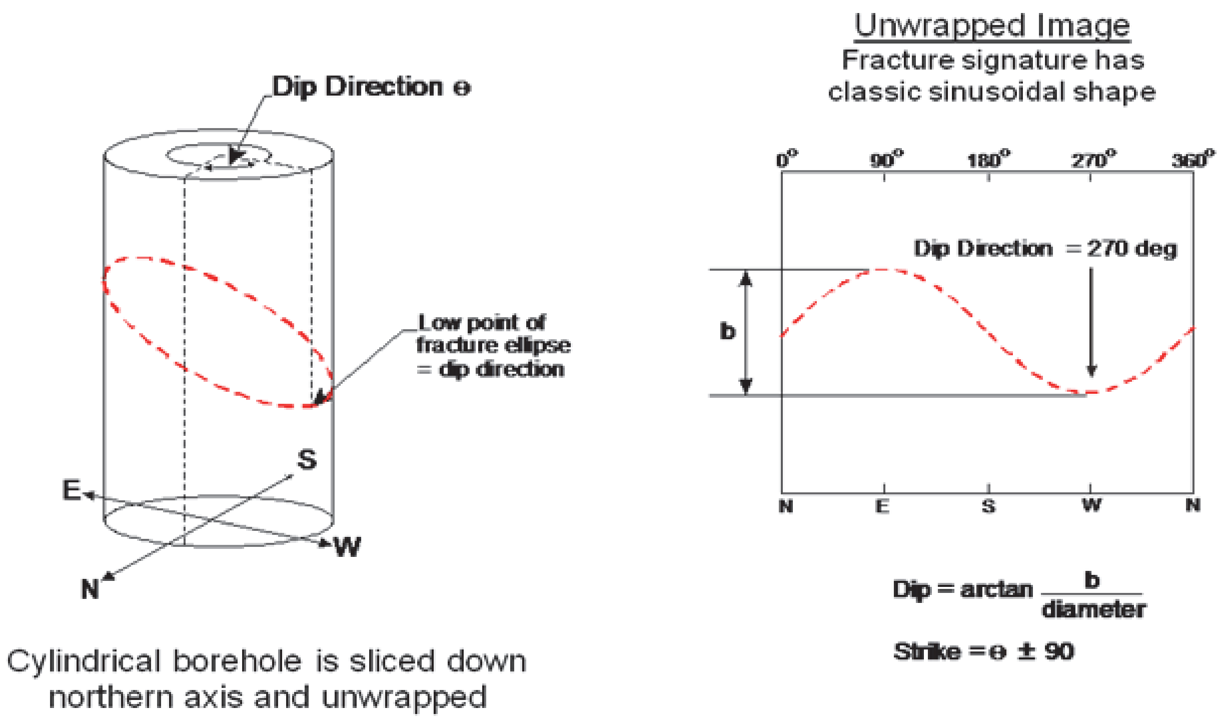


Figure A- 6: Schematic showing the sinusoidal fracture signature in the unwrapped borehole view.

## ACOUSTIC TELEVIEWER (ATV) LOGS

Acoustic televiewer provides a 360° acoustic image of the borehole walls that can be used to identify and determine the orientation of planar features such as bedding and fractures. The data can also indicate the relative degree of hardness of formation materials. As shown in Figure A-7, Ultrasonic pulses are transmitted from a rotating transducer inside the tool. The transmitted pulses reflect off the borehole wall and return to the tool where the travel time and amplitude of the acoustic signal are measured. In order for the acoustic waves to travel to and from the borehole wall, the well must be fluid filled. Greater travel time can indicate openings in the rock. Strong amplitude suggests smooth, competent rock. Weaker amplitudes suggest rough or less competent rock.

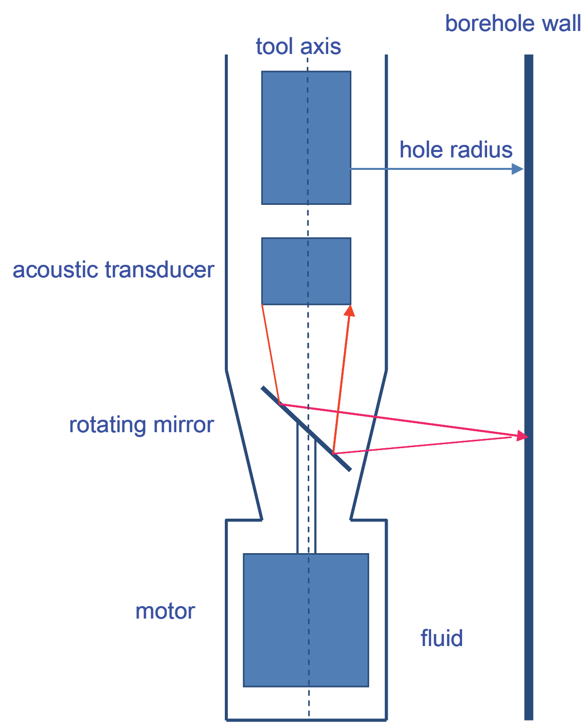


**Figure A- 7: Schematic of the acoustic televiewer tool.**

## DENSITY LOGS

Density logs are most often used to determine formation porosity. The probe uses a radioactive source capsule (typically containing cesium) to bombard the formation with low energy gamma rays. These rays can be thought of as particles that collide with the electrons in the formation. As these particles collide, the gamma rays are attenuated or lose energy. This loss of energy, called Compton Scattering, is directly related to the number of electrons in the formation. Therefore, the tool responds to electron density which is linearly related to bulk density. Bulk density in turn, is related to the density of the rock matrix material, the porosity of the formation, and the density of the fluids filling the pores. The density ranges for common rock types is shown below:

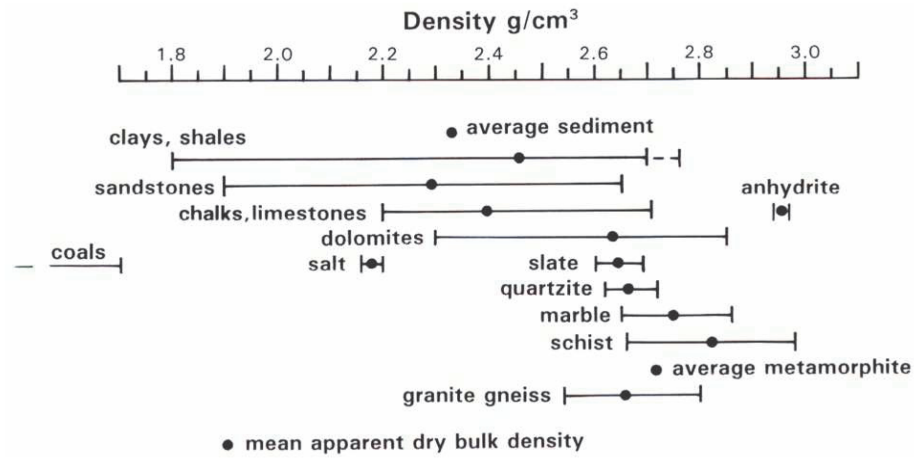


The density of the matrix materials and pore fluids must be known or estimated to calculate formation porosity. The porosity of the formation can be determined by:

$$\phi_{density} = \frac{\rho_{ma} - \rho_b}{\rho_{ma} - \rho_f}$$

Where: $\rho_{ma}$ = matrix density
$\rho_b$ = bulk density
$\rho_f$ = fluid density

Densities for common matrix lithologies and fluid type are shown below:

| Material | Density |
|---|---|
| Sandstone | 2.65 g/cm3 |
| Limestone | 2.71 g/cm3 |
| Dolomite | 2.87 g/cm3 |
| Fresh water | 1.00 g/cm3 |
| Salt water (200g/l) | 1.13 g/cm3 |
| Fresh water + 30% oil | 0.73 - 0.78 g/cm3 |

## NEUTRON LOGS

Neutron logs are typically used to identify porous formations and determine their porosity. Neutron tools use a sealed radioactive source such as americium-beryllium to measure the amount of hydrogen in a formation. Fast neutrons are emitted from the tool and bombard the formation, causing collisions with the nuclei of formation materials. These collisions attenuate the neutron energy. The greatest amount of energy is lost when particles of nearly equal mass collide. Neutrons have a mass almost identical to hydrogen. Thus the attenuation of neutron energy is largely controlled by the amount of hydrogen in the formation.

Since water and oil contain a lot of hydrogen, the tool response reflects the liquid-filled porosity in clay-free formations such as sandstone and limestone. However, shales contain bound water in its crystal structure that will produce higher apparent porosity than the actual effective porosity of the formation. For this reason it is important to interpret the results in conjunction with the gamma ray log, which is good indicator of clay/shale volume.

## SONIC LOGS

Sonic logs are typically used to help identify lithology, porosity, and mechanical rock properties. The sonic tool contains acoustic transmitters and receivers. A sound pulse is generated by a transmitter and travels through the formation. One or more receivers record the sound pulse as it passes. The sonic log is simply a record of the time interval at which sound travels through 1 ft of formation. This measurement is called the interval transit time, slowness, or delta t ($\Delta t$) and is the reciprocal of the velocity of the sound wave.

As the sound wave emitted by the transmitter encounters the borehole wall, 1) compressional and shear waves are generated in the formation, 2) surface wave along the borehole wall, and 3) tube waves in the borehole fluid. The first and second sound wave arrivals at the receiver are the compressional (P-wave) and shear (S-wave) arrivals, respectively. These are the most common signals used in sonic logging and their transit times vary with lithology and porosity. In addition, the interrelationship between the S- and P-waves and density can be used to calculate mechanical rock properties such as Poisson’s ratio, bulk modulus, Young’s modulus, and shear modulus.

Sonic-derived porosity is given by:

$$\phi_{sonic} = \frac{\Delta t_{\log} - \Delta t_{ma}}{\Delta t_f - \Delta t_{ma}}$$

Where:

$\phi_{sonic}$ = sonic derived porosity

$\Delta t_{ma}$ = interval transit time (compressional) for matrix

$\Delta t_f$ = interval transit time for borehole fluid

The interval transit times for common materials are shown below:

| Material | $\Delta t_{ma}$ msec/ft |
|---|---|
| Sandstone | 55.5 |
| Limestone | 47.6 |
| Dolomite | 43.5 |
| Water + 20% NaCl | 189 |
| Water + 10% NaCl | 208 |
| Water (pure) | 218 |

Engineering mechanical rock properties are calculated using the shear and compressional interval travel times measured by the sonic log and bulk density measured by the gamma density log. The following engineering properties can be calculated from these logs:

- **Shear Modulus ($\mu$)** also called rigidity modulus, measures the opposition of a substance to shear stresses.

$$\mu = C \frac{\rho_b}{\Delta t_s^{\,2}}$$

$\mu =$ Shear Modulus
$C =$ Constant $(1.34 \; *10^{10})$
$\rho_b =$ Bulk Density
$\Delta t_s =$ Shear wave transit time $\cong \Delta t_c * 1.75$
$\Delta t_c =$ Compressional wave transit time

- **Young's modulus (E)** measures opposition of a substance to extensional stress.

$$E = \left(\frac{\rho_b}{\Delta t_s^{\,2}}\right)\left(\frac{3\Delta t_s^{\,2} - 4\Delta t_c^{\,2}}{\Delta t_s^{\,2} - \Delta t_c^{\,2}}\right) C$$

- **Bulk modulus (K)** is the coefficient of incompressibility and measures opposition of substance to compressional stress.

$$K = \rho_b \left(\frac{3\Delta t_s^{\,2} - 4\Delta t_c^{\,2}}{3\Delta t_s^{\,2} \Delta t_c^{\,2}}\right) C$$

- **Poisson's Ratio (σ)** is the ratio of relative decrease in diameter to relative elongation.

$$\sigma = 1/2\left(\frac{\Delta t_s{}^2 - 2\Delta t_c{}^2}{\Delta t_s{}^2 - \Delta t_c{}^2}\right)C$$

# ATTACHMENT B
# BOREHOLE LOGS

# Fluid Temperature
# Fluid Conductivity
# Natural Gamma

| | |
|---|---|
| COMP | Penn State University |
| WELL | CZMW-4 |
| FLD | Petersburg |
| CNTY | Huntingdon |
| STAT | PA |
| ARM | 170597 |
| API | N/A |

| | | | |
|---|---|---|---|
| COMPANY: | Penn State University | STATE: | PA |
| WELL ID: | CZMW-4 | ARM NO.: | 170597 |
| FIELD/SITE: | Petersburg | API NO.: | N/A |
| COUNTY: | Huntingdon | | |

LOCATION: OTHER SERVICES
NORTHING:
EASTING:
SEC: TWP: QUAD:

PERMANENT DATUM: Ground Surface ELEVATION: K.B.
LOG MEASURED FROM: Ground Surface ABOVE PERM. DATUM: D.F.
DRILLING MEAS. FROM: STICK UP: 1.0 G.L.

| | | | | | |
|---|---|---|---|---|---|
| LOGGING DATE | 11.21.2017 | | | | |
| RUN NO | 1 | | | | |
| TYPE LOG | FTC.GR | | | | |
| DRILLER DEPTH (FT) | 50 | | | | |
| ARM DEPTH (FT) | 49.1 | | | | |
| BTM LOGGED INTERVAL (FT) | 49.47 | | | | |
| TOP LOGGED INTERVAL (FT) | 5.13 | | | | |
| CASING SIZE (IN)/DEPTH (FT) | 2/* | | | | |
| CASING ARM (FT) | * | | | | |
| BIT SIZE (IN) | | | | | |
| FLUID LEVEL IN HOLE (FT) | ** | | | | |
| MAG. DECLINATION (DEG) | 10.65 W | | | | |
| RECORDED BY | R. Gecelosky | | | | |
| WITNESSED BY | D. Rajkovic | | | | |

REMARKS:
*Cased to the bottom of the borehole.
**Artisian

**Symbols**

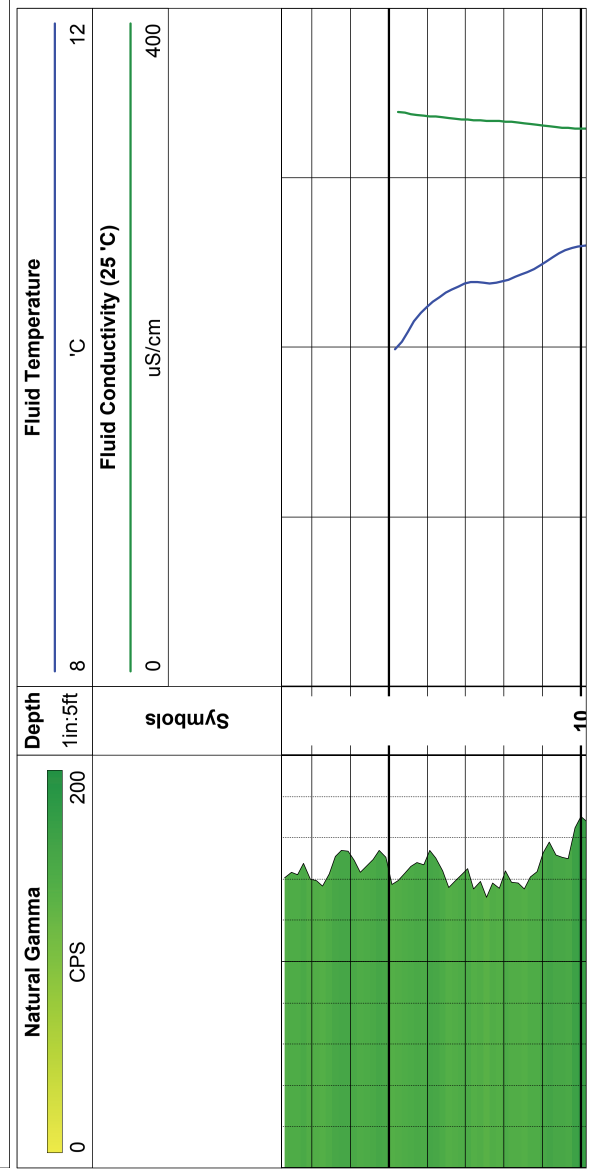

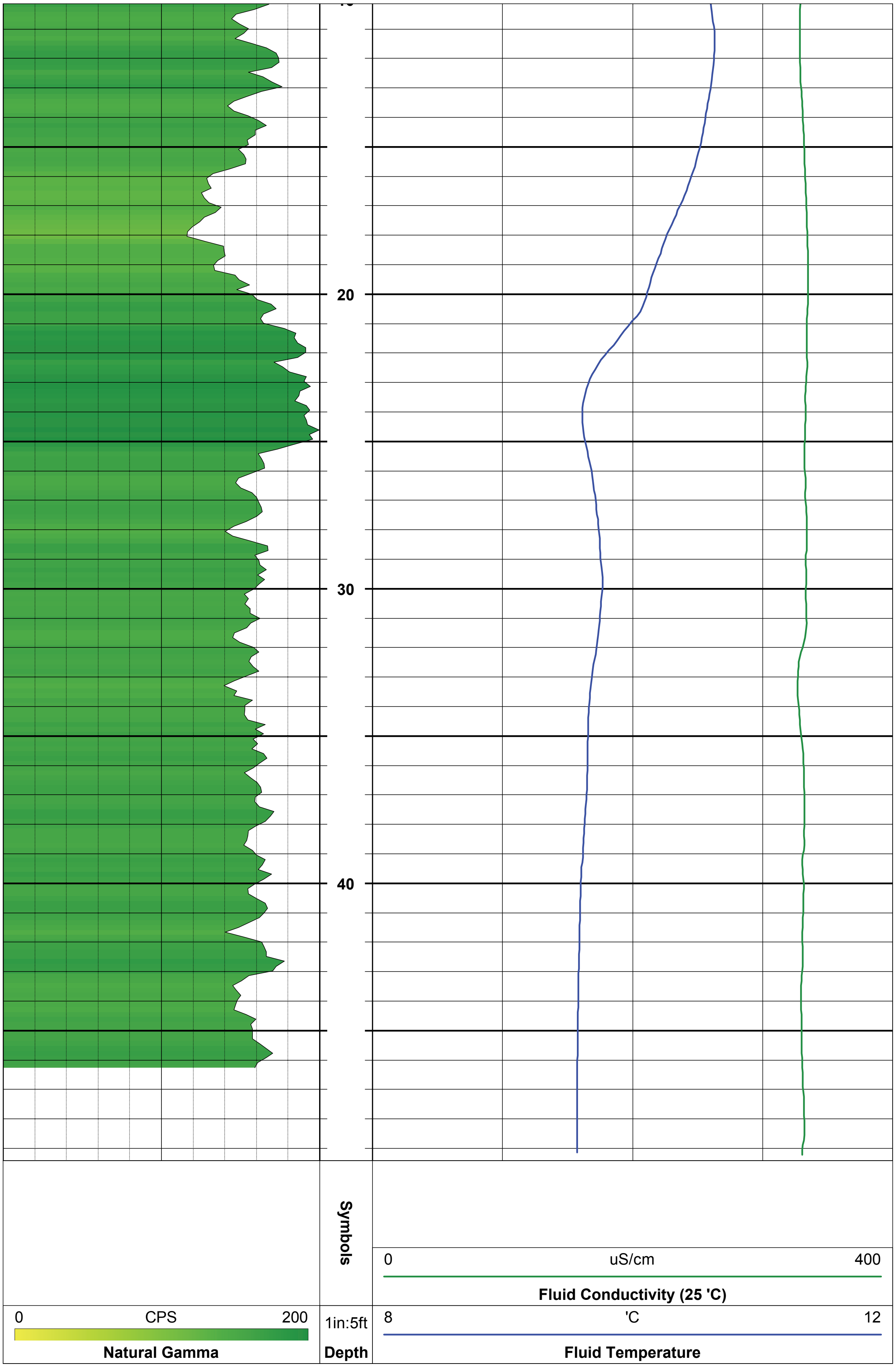
20
30
40
Symbols
0
uS/cm
400
Fluid Conductivity (25 'C)
0
CPS
200
Natural Gamma
1in:5ft
Depth
8
'C
12
Fluid Temperature

# Televiewer Logs

| | |
|---|---|
| COMP | Penn State University |
| WELL | CZMW-10 |
| FLD | Petersburg |
| CNTY | Huntingdon |
| STAT | PA |
| ARM | 170597 |
| API | N/A |

COMPANY: Penn State University STATE: PA
WELL ID: CZMW-10 ARM NO.: 170597
FIELD/SITE: Petersburg API NO.: N/A
COUNTY: Huntingdon
LOCATION: Scare Pond Road
NORTHING:
EASTING:
SEC: TWP: QUAD:

OTHER SERVICES

PERMANENT DATUM: Ground Surface ELEVATION: K.B.
LOG MEASURED FROM: Ground Surface ABOVE PERM. DATUM: 0.00 D.F.
DRILLING MEAS. FROM: STICK UP: 0.94 G.L.

| | | | | | |
|---|---|---|---|---|---|
| LOGGING DATE | 11.21.2017 | 11.21.2017 | | | |
| RUN NO | 2 | 4 | | | |
| TYPE LOG | OTV | ATV | | | |
| DRILLER DEPTH (FT) | 115.0 | 115.0 | | | |
| ARM DEPTH (FT) | 114.7 | 114.9 | | | |
| BTM LOGGED INTERVAL (FT) | 114.9 | 114.9 | | | |
| TOP LOGGED INTERVAL (FT) | 6.2 | 6.0 | | | |
| CASING SIZE (IN)/DEPTH (FT) | 4.0/40.0 | 4.0/40.0 | | | |
| CASING ARM (FT) | 40.4 | 40.4 | | | |
| BIT SIZE (IN) | | | | | |
| FLUID LEVEL IN HOLE (FT) | 0.0 | 0.0 | | | |
| MAG. DECLINATION (DEG) | 10.65 W | 10.65 W | | | |
| RECORDED BY | R. Gecelosky | R. Gecelosky | | | |
| WITNESSED BY | D. Rajkovic | D. Rajkovic | | | |

REMARKS:

## Symbols

Bottom of Casing

## Structure

Open Fracture
Bedding
Discontinuous Fract
Part. Open Fract
Filled Fracture

| Optical Image | Depth | Acoustic Amplitude | Acoustic Travel Time | Plane Projection | Dip & Dip Direction |
|---|---|---|---|---|---|
| 0° 90° 180° 270° 0° | 1in:2ft | 0° 90° 180° 270° 0° | 0° 90° 180° 270° 0° | 0° 90° 180° 270° 0° | 0 90 |
| | Symbols | | | | |

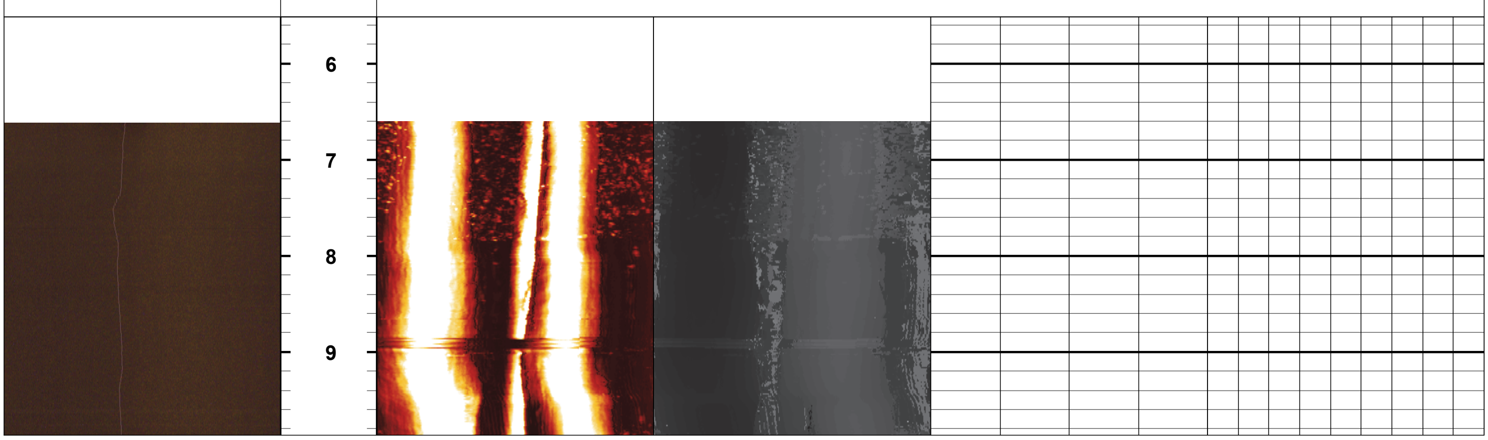

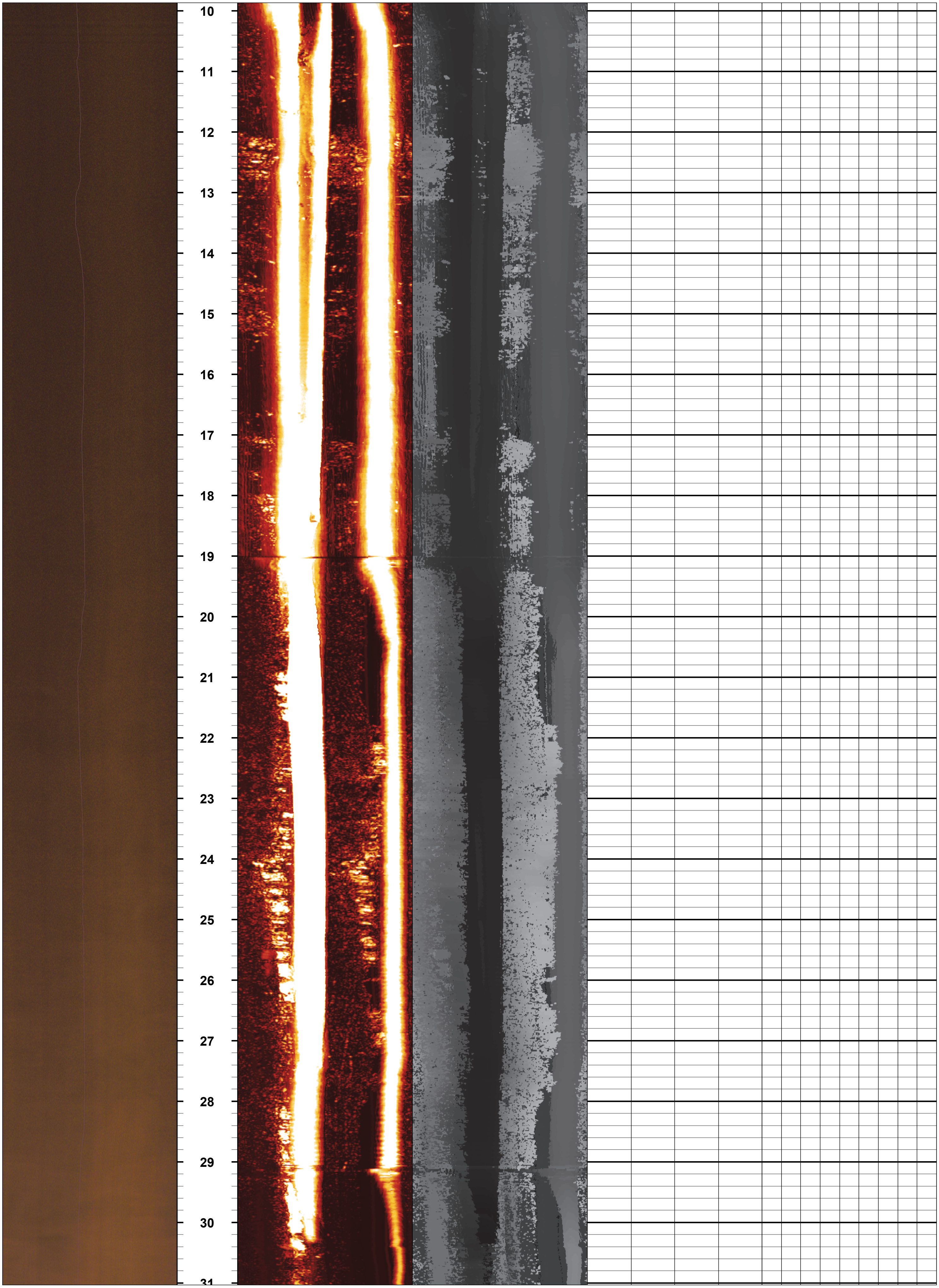
10
11
12
13
14
15
16
17
18
19
20
21
22
23
24
25
26
27
28
29
30
31

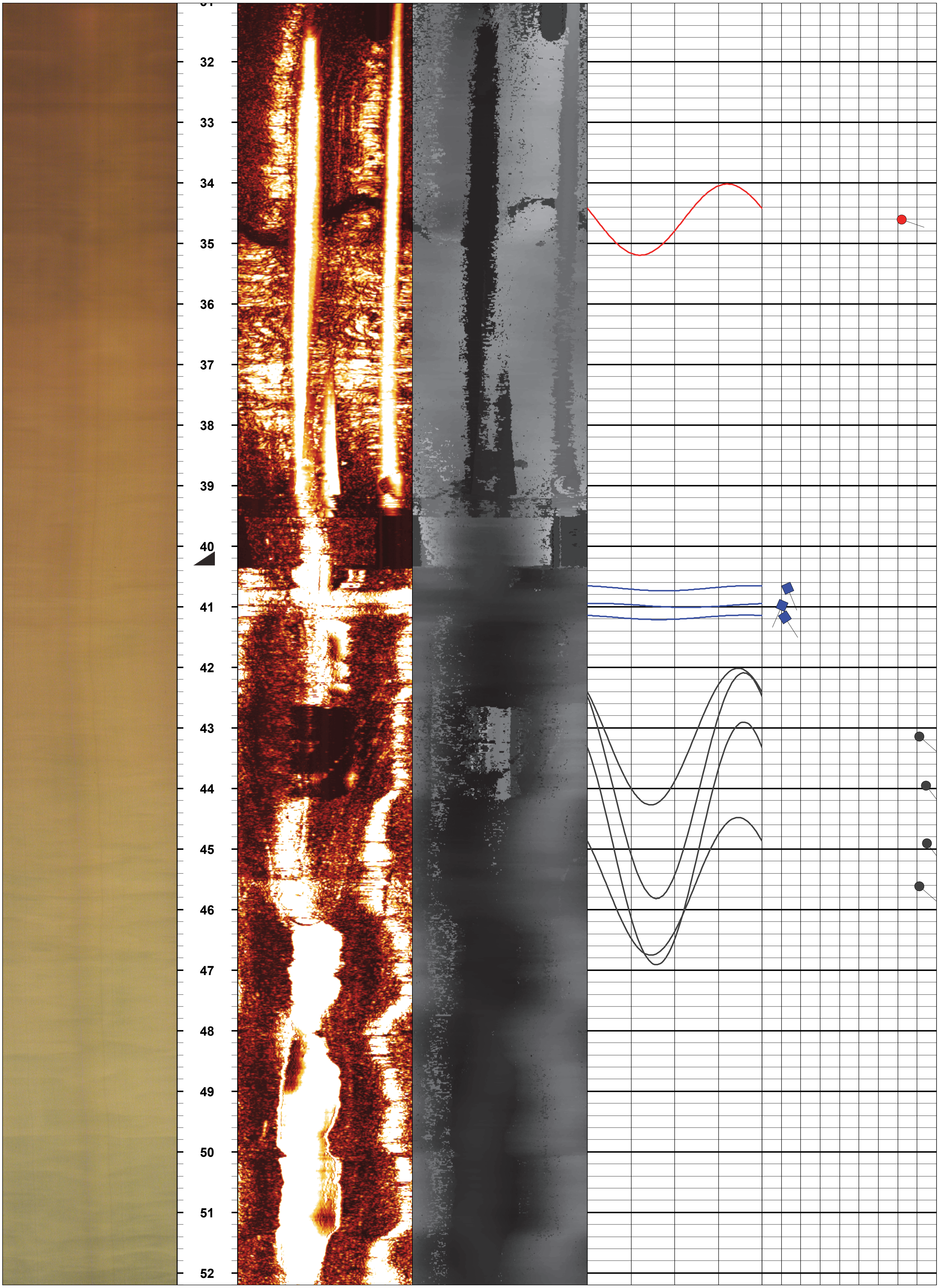
32
33
34
35
36
37
38
39
40
41
42
43
44
45
46
47
48
49
50
51
52

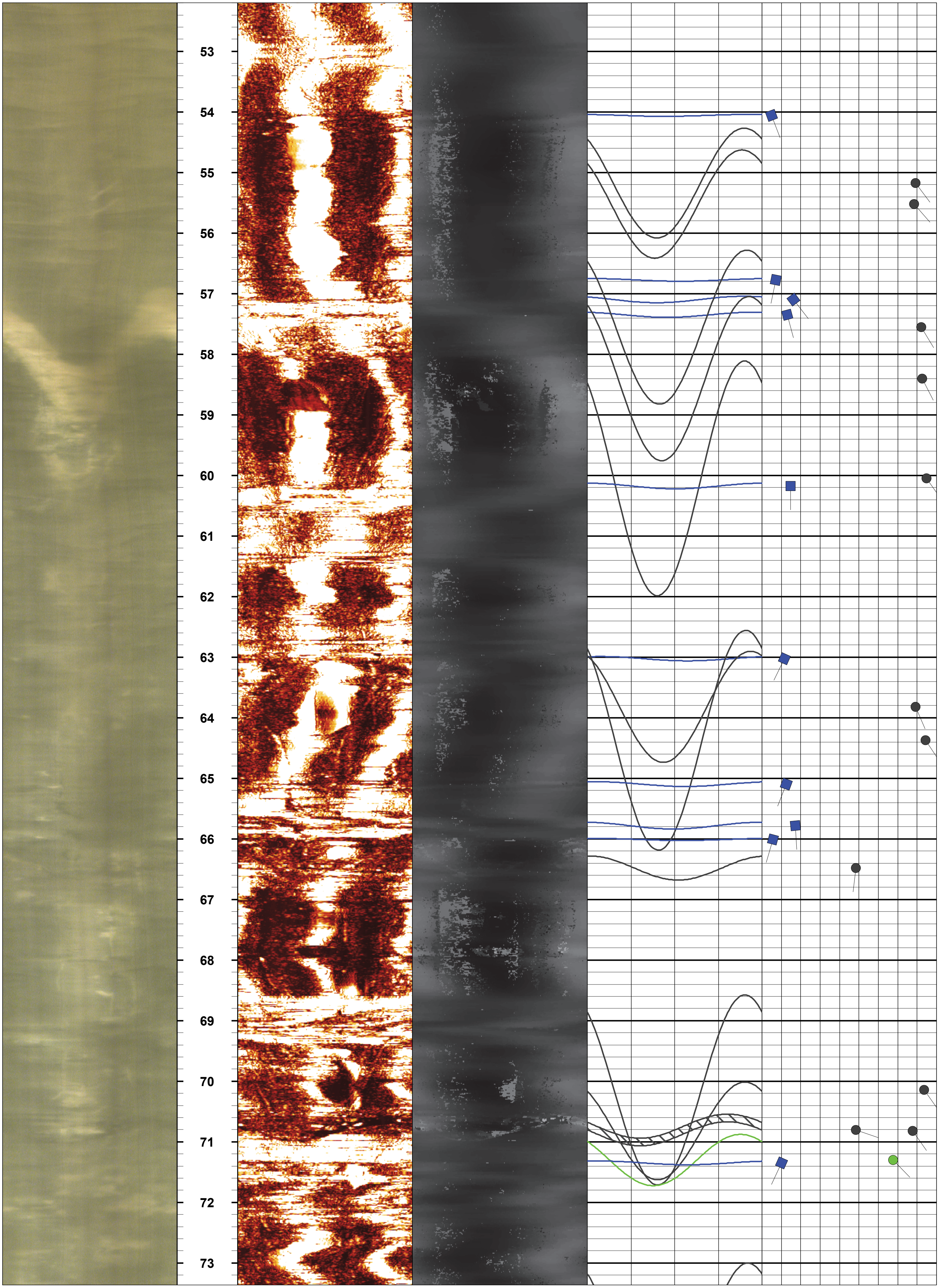
53
54
55
56
57
58
59
60
61
62
63
64
65
66
67
68
69
70
71
72
73

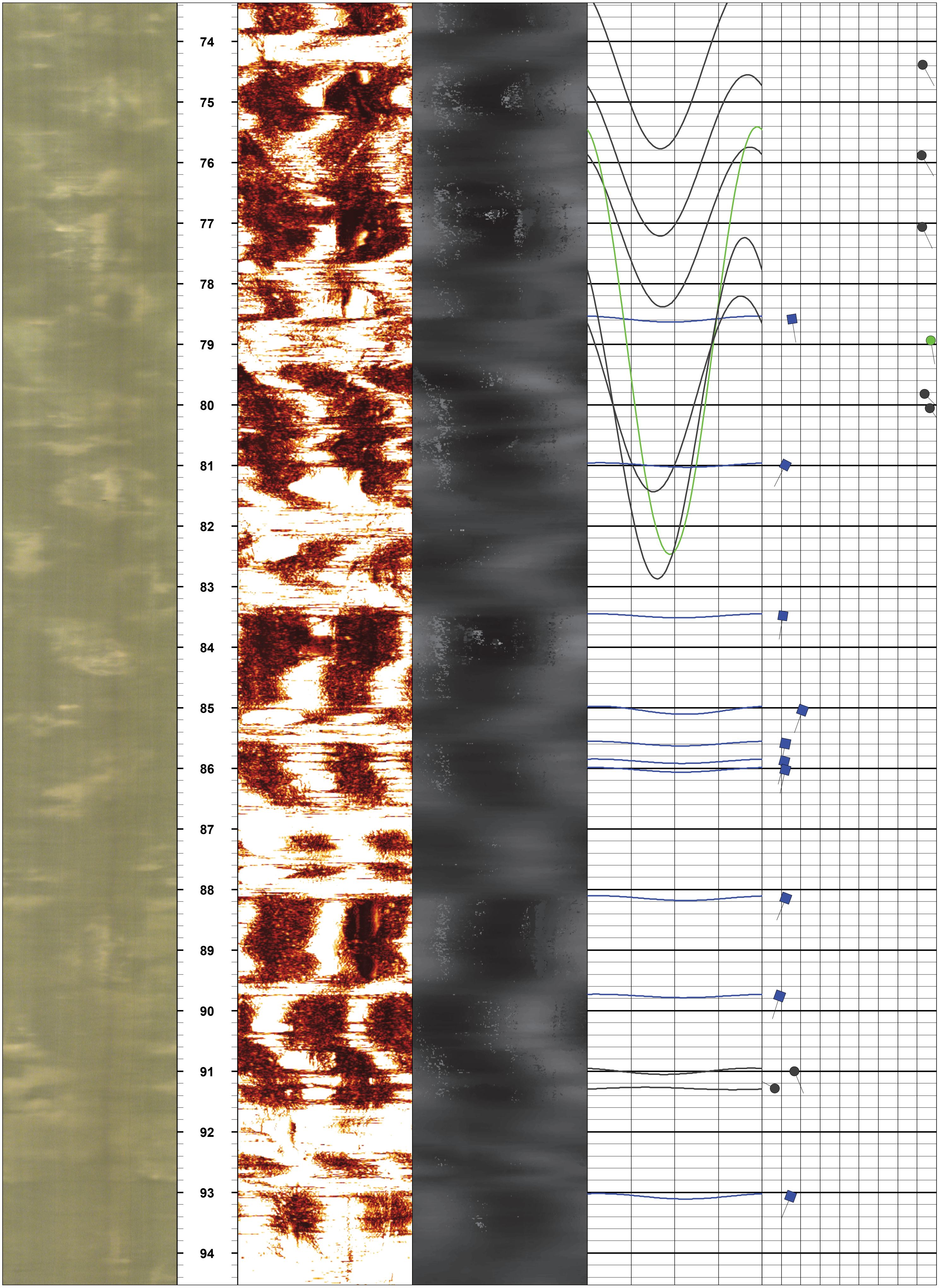
74
75
76
77
78
79
80
81
82
83
84
85
86
87
88
89
90
91
92
93
94

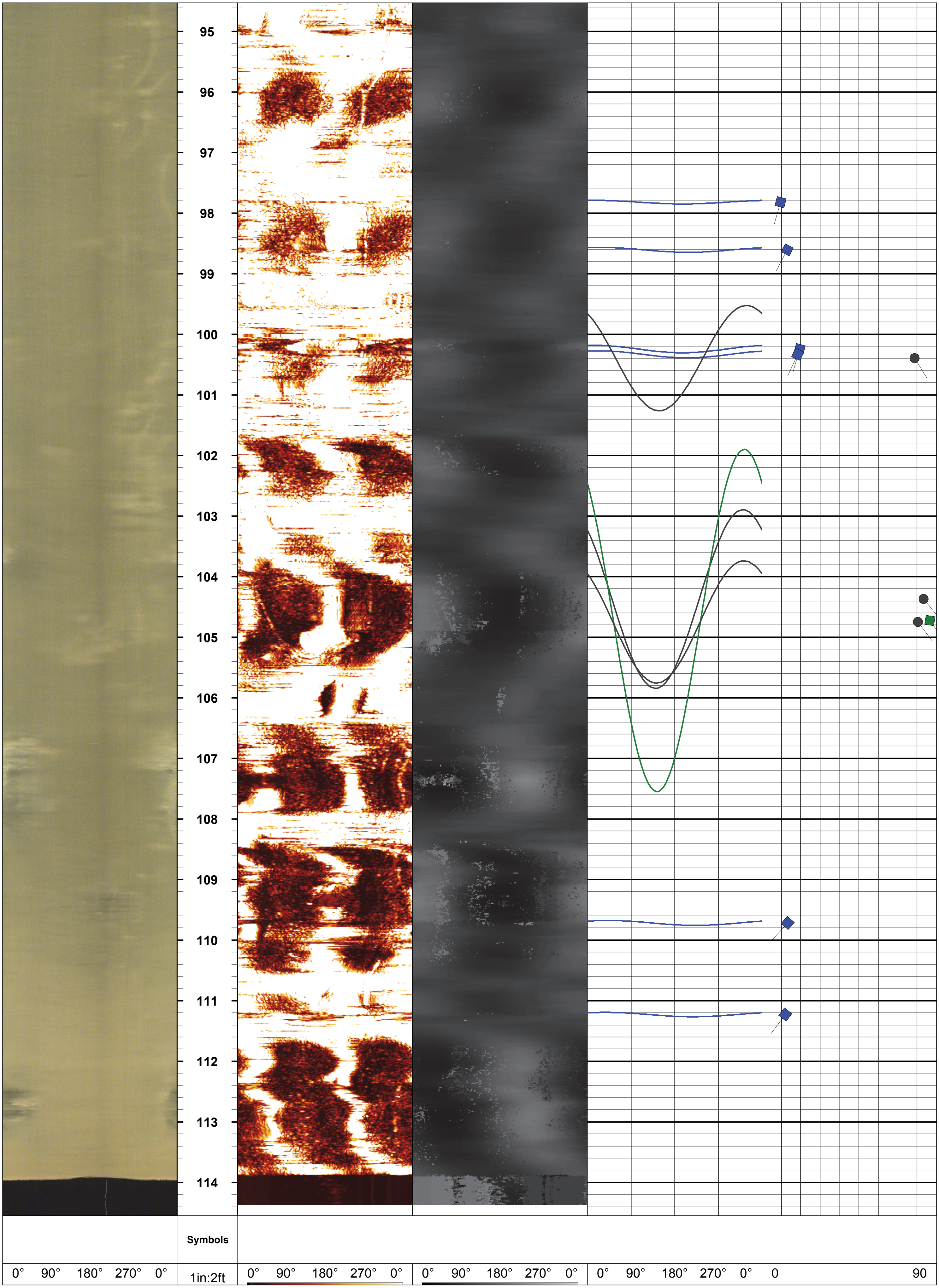
95
96
97
98
99
100
101
102
103
104
105
106
107
108
109
110
111
112
113
114
Symbols
0° 90° 180° 270° 0°
1in:2ft
0° 90° 180° 270° 0°
0° 90° 180° 270° 0°
0° 90° 180° 270° 0°
0
90

| Optical Image | Depth | Acoustic Amplitude | Acoustic Travel Time | Plane Projection | Dip & Dip Direction |
|---|---|---|---|---|---|

# Hydro Log

ARM GEOPHYSICS — Surface & Borehole Services

| | |
|---|---|
| COMP | **Penn State University** |
| WELL | **CZMW-10** |
| FLD | **Petersburg** |
| CNTY | **Huntingdon** |
| STAT | **PA** |
| ARM | **170597** |
| API | **N/A** |

COMPANY: Penn State University — STATE: PA
WELL ID: CZMW-10 — ARM NO.: 170597
FIELD/SITE: Petersburg — API NO.: N/A
COUNTY: Huntingdon
LOCATION: Scare Pond Road — OTHER SERVICES
NORTHING:
EASTING:
SEC: — TWP: — QUAD:

PERMANENT DATUM: Ground Surface — ELEVATION: — K.B.
LOG MEASURED FROM: Ground Surface — ABOVE PERM. DATUM: 0.00 — D.F.
DRILLING MEAS. FROM: — STICK UP: 0.94 — G.L.

| | | | | | |
|---|---|---|---|---|---|
| LOGGING DATE | 11.21.2017 | 11.21.2017 | 11.21.2017 | 11.21.2017 | 11.21.2017 |
| RUN NO | 1 | 3 | 5 | 6 | 7 |
| TYPE LOG | FTC.GR | CAL | RES | NEU | DEN |
| DRILLER DEPTH (FT) | 115.0 | 115.0 | 115.0 | 115.0 | 115.0 |
| ARM DEPTH (FT) | 114.9 | 115.0 | 115.0 | 114.5 | 114.8 |
| BTM LOGGED INTERVAL (FT) | 115.2 | 115.0 | 115.0 | 114.5 | 114.8 |
| TOP LOGGED INTERVAL (FT) | 6.2 | 6.7 | 6.0 | 11.0 | 13.7 |
| CASING SIZE (IN)/DEPTH (FT) | 4.0/40.0 | 4.0/40.0 | 4.0/40.0 | 4.0/40.0 | 4.0/40.0 |
| CASING ARM (FT) | 40.4 | 40.4 | 40.4 | 40.4 | 40.4 |
| BIT SIZE (IN) | | | | | |
| FLUID LEVEL IN HOLE (FT) | 0.0 | 0.0 | 0.0 | 0.0 | 0.0 |
| MAG. DECLINATION (DEG) | 10.65 W | 10.65 W | 10.65 W | 10.65 W | 10.65 W |
| RECORDED BY | R. Gecelosky | R. Gecelosky | R. Gecelosky | R. Gecelosky | R. Gecelosky |
| WITNESSED BY | D. Rajkovic | D. Rajkovic | D. Rajkovic | D. Rajkovic | D. Rajkovic |

REMARKS:
Run No 8, FWS - 2SAA(F)
T1:M-D, 7KHz 1@50ms
RX1:M, 100uS,256@

**Symbols**

| Track | Curve | Left | Units | Right |
|---|---|---|---|---|
| 1 | Natural Gamma | 0 | CPS | 200 |
| 1 | 3-Arm Caliper | 3 | in | 6 |
| 1 | Spontaneous Potential | 0 | mV | 500 |
| 1 | Single Point Resistance | 0 | Ohm | 500 |
| 1 | P-Wave Velocity | 3000 | ft/s | 16000 |
| 1 | S-Wave Velocity | 3000 | ft/s | 16000 |
| Depth | Depth | | 1in:5ft | |
| Symbols | Symbols | | | |
| Televiewer Fractures | Televiewer Fractures | | | |
| 2 | Fluid Temperature | 10 | 'C | 15 |
| 2 | Fluid Conductivity | 200 | uS/cm | 400 |
| 2 | Normal Resistivity - 8-inch | 20 | Ohm.m | 2000 |
| 2 | Normal Resistivity - 64-inch | 20 | Ohm.m | 2000 |
| 2 | Neutron Porosity | 0.3 | PU | -0.1 |
| 2 | BulkDensity | 1 | g/cc | 3 |
| 3 | Velocity Analysis | 0 | us/ft | 417.6 |
| 3 | P-wave Slowness | 0 | us/ft | 417.6 |
| 3 | S-Wave Slowness | 0 | us/ft | 417.6 |

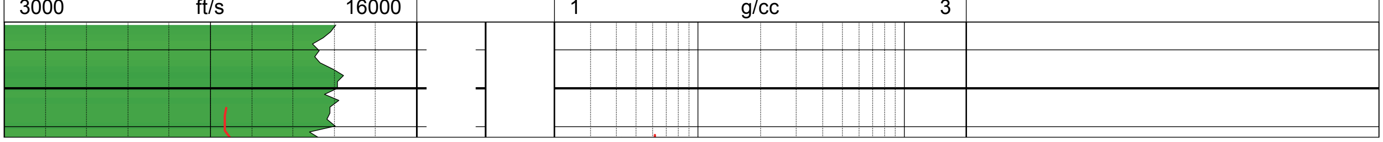

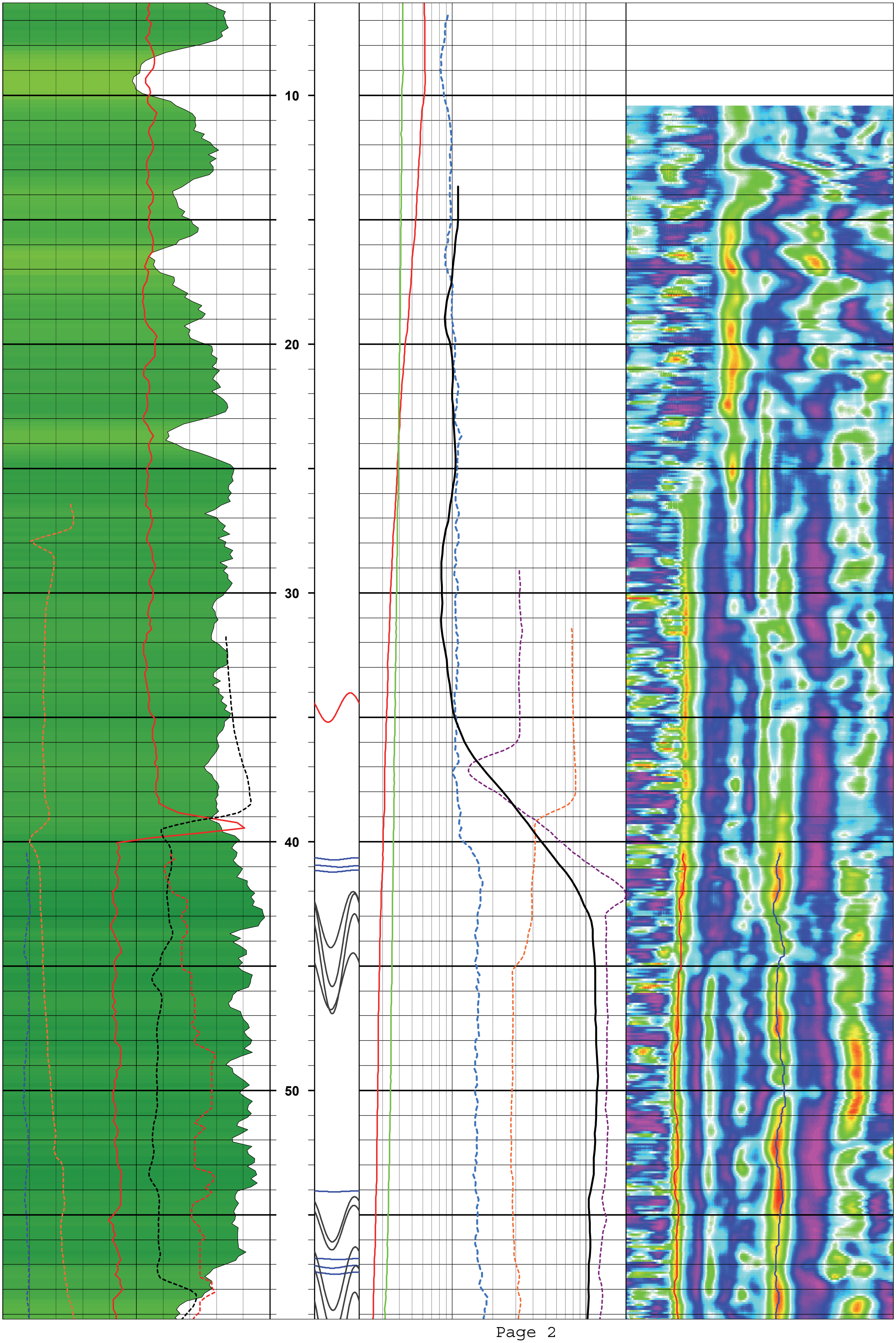
10
20
30
40
50

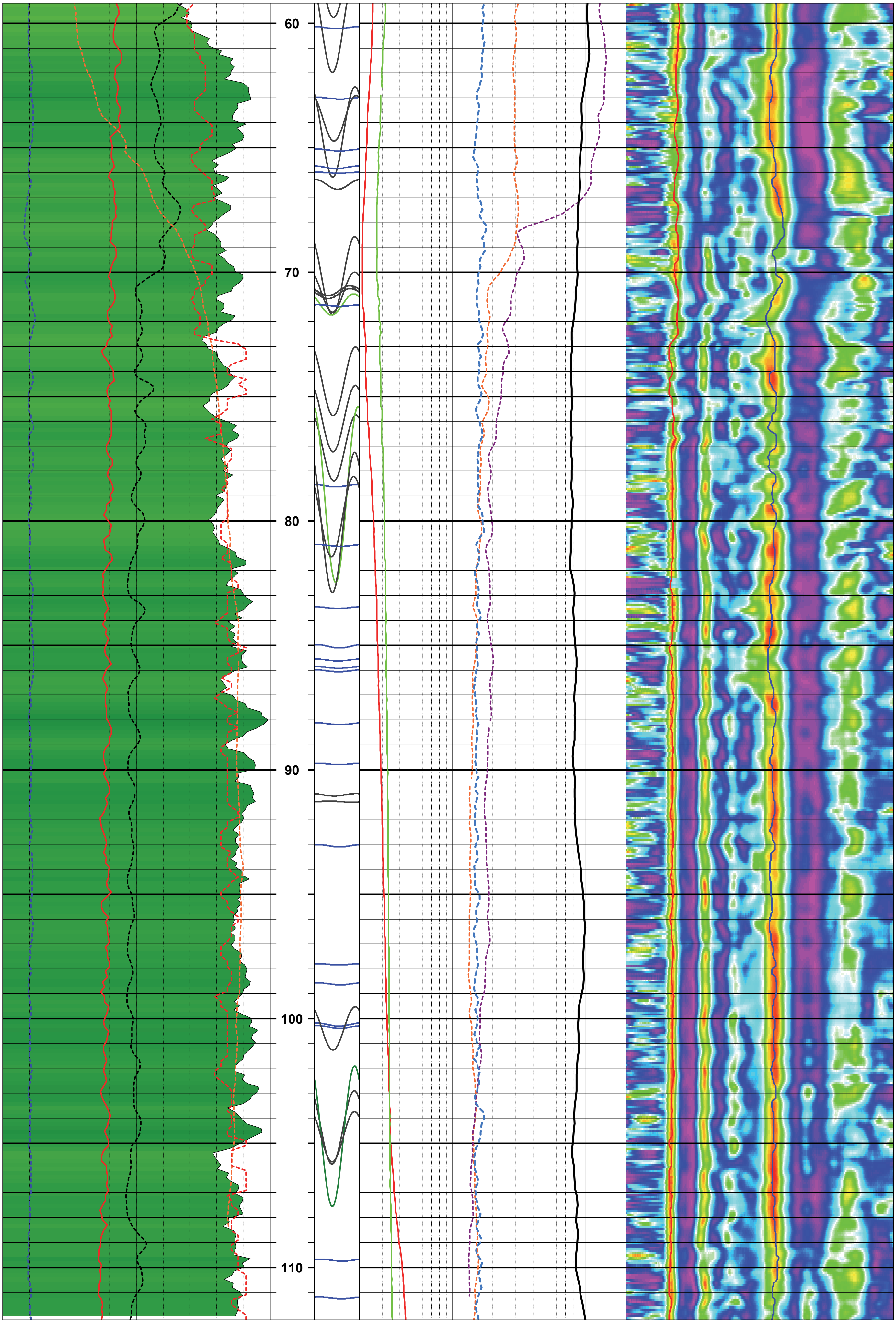
60
70
80
90
100
110

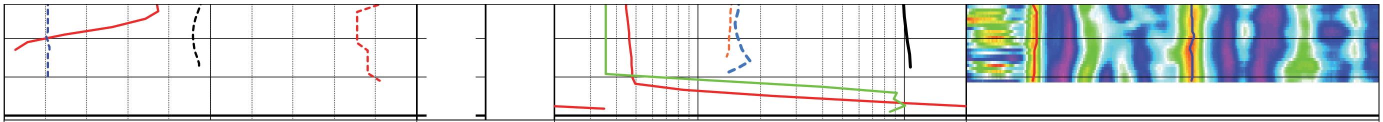

| | | | | |
|---|---|---|---|---|
| 3000 ft/s 16000 **S-Wave Velocity** | | | 1 g/cc 3 **BulkDensity** | |
| 3000 ft/s 16000 **P-Wave Velocity** | | | 0.3 PU -0.1 **Neutron Porosity** | |
| 0 Ohm 500 **Single Point Resistance** | **Symbols** | **Televiewer Fractures** | 20 Ohm.m 2000 **Normal Resistivity - 64-inch** | |
| 0 mV 500 **Spontaneous Potential** | | | 20 Ohm.m 2000 **Normal Resistivity - 8-inch** | **0 us/ft 417.6** **S-Wave Slowness** |
| 3 in 6 **3-Arm Caliper** | | | 200 uS/cm 400 **Fluid Conductivity** | **0 us/ft 417.6** **P-wave Slowness** |
| 0 CPS 200 **Natural Gamma** | 1in:5ft **Depth** | | 10 'C 15 **Fluid Temperature** | 0 us/ft 417.6 **Velocity Analysis** |

# ATTACHMENT C
# TABULATED LISTING OF PLANE ORIENTATIONS

# Planar Orientations

| Well ID | Depth (feet) | Dip Dir. (deg) | Dip (deg) | Aperture (mm) | Type | Strike/Dip (Quadrant) |
|---|---|---|---|---|---|---|
| CZMW-10 | 34.61 | 108.44 | 72.04 | 0 | Open Fracture | N18E/72SE |
| CZMW-10 | 40.69 | 157.75 | 13.4 | 0 | Bedding | N68E/13SE |
| CZMW-10 | 40.98 | 203.89 | 10.35 | 0 | Bedding | N66W/10SW |
| CZMW-10 | 41.17 | 147.57 | 11.78 | 0 | Bedding | N58E/12SE |
| CZMW-10 | 43.14 | 130.73 | 81.2 | 0 | Part. Open Fract | N41E/81SE |
| CZMW-10 | 43.95 | 142.38 | 84.57 | 0 | Part. Open Fract | N52E/85SE |
| CZMW-10 | 44.9 | 142.33 | 85.02 | 0 | Part. Open Fract | N52E/85SE |
| CZMW-10 | 45.61 | 130.96 | 81.15 | 0 | Part. Open Fract | N41E/81SE |
| CZMW-10 | 54.06 | 159.2 | 4.99 | 0 | Bedding | N69E/5SE |
| CZMW-10 | 55.17 | 143.18 | 79.1 | 0 | Part. Open Fract | N53E/79SE |
| CZMW-10 | 55.52 | 138.77 | 78.55 | 0 | Part. Open Fract | N49E/79SE |
| CZMW-10 | 56.77 | 191.32 | 7.06 | 0 | Bedding | N79W/7SW |
| CZMW-10 | 57.09 | 142.25 | 16.27 | 0 | Bedding | N52E/16SE |
| CZMW-10 | 57.35 | 164.69 | 12.99 | 0 | Bedding | N75E/13SE |
| CZMW-10 | 57.55 | 148.45 | 82.07 | 0 | Part. Open Fract | N58E/82SE |
| CZMW-10 | 58.4 | 153.18 | 82.67 | 0 | Part. Open Fract | N63E/83SE |
| CZMW-10 | 60.05 | 144.21 | 84.77 | 0 | Part. Open Fract | N54E/85SE |
| CZMW-10 | 60.17 | 180.51 | 14.79 | 0 | Bedding | N89W/15SW |
| CZMW-10 | 63.02 | 205.83 | 11.57 | 0 | Bedding | N64W/12SW |
| CZMW-10 | 63.82 | 156.51 | 79.06 | 0 | Part. Open Fract | N67E/79SE |
| CZMW-10 | 64.37 | 146.58 | 84.38 | 0 | Part. Open Fract | N57E/84SE |
| CZMW-10 | 65.09 | 201.66 | 12.64 | 0 | Bedding | N68W/13SW |
| CZMW-10 | 65.78 | 176.3 | 17.3 | 0 | Bedding | N86E/17SE |
| CZMW-10 | 66.01 | 195.71 | 5.54 | 0 | Bedding | N74W/6SW |
| CZMW-10 | 66.48 | 187.05 | 48.45 | 0 | Part. Open Fract | N83W/48SW |
| CZMW-10 | 70.14 | 144.97 | 83.6 | 0 | Part. Open Fract | N55E/84SE |
| CZMW-10 | 70.8 | 108.61 | 48.51 | 9.69 | Part. Open Fract | N19E/49SE |
| CZMW-10 | 70.82 | 144.59 | 77.67 | 0 | Part. Open Fract | N55E/78SE |
| CZMW-10 | 71.3 | 135.85 | 67.59 | 0 | Discontinuous Fract | N46E/68SE |
| CZMW-10 | 71.35 | 205.34 | 10.09 | 0 | Bedding | N65W/10SW |
| CZMW-10 | 74.39 | 150.67 | 82.76 | 0 | Part. Open Fract | N61E/83SE |
| CZMW-10 | 75.88 | 149.56 | 82.42 | 0 | Part. Open Fract | N60E/82SE |
| CZMW-10 | 77.07 | 155.21 | 82.52 | 0 | Part. Open Fract | N65E/83SE |
| CZMW-10 | 78.58 | 170.69 | 15.6 | 0 | Bedding | N81E/16SE |
| CZMW-10 | 78.94 | 170.39 | 87.1 | 0 | Discontinuous Fract | N80E/87SE |
| CZMW-10 | 79.82 | 136.35 | 83.93 | 0 | Part. Open Fract | N46E/84SE |
| CZMW-10 | 80.05 | 144.1 | 86.48 | 0 | Part. Open Fract | N54E/86SE |
| CZMW-10 | 80.99 | 207.07 | 12.03 | 0 | Bedding | N63W/12SW |
| CZMW-10 | 83.48 | 188.97 | 10.9 | 0 | Bedding | N81W/11SW |
| CZMW-10 | 85.04 | 199.54 | 20.96 | 0 | Bedding | N70W/21SW |
| CZMW-10 | 85.59 | 191.29 | 12.06 | 0 | Bedding | N79W/12SW |
| CZMW-10 | 85.88 | 194.81 | 11.46 | 0 | Bedding | N75W/11SW |
| CZMW-10 | 86.03 | 193.06 | 12.09 | 0 | Bedding | N77W/12SW |
| CZMW-10 | 88.14 | 202.02 | 12.41 | 0 | Bedding | N68W/12SW |
| CZMW-10 | 89.76 | 198.02 | 9.01 | 0 | Bedding | N72W/9SW |
| CZMW-10 | 91 | 157.73 | 16.64 | 0 | Part. Open Fract | N68E/17SE |
| CZMW-10 | 91.29 | 299.12 | 6.63 | 0 | Part. Open Fract | N29E/7NW |
| CZMW-10 | 93.06 | 201.76 | 14.68 | 0 | Bedding | N68W/15SW |
| CZMW-10 | 97.82 | 196.79 | 9.66 | 0 | Bedding | N73W/10SW |
| CZMW-10 | 98.61 | 207.49 | 13.14 | 0 | Bedding | N63W/13SW |
| CZMW-10 | 100.25 | 195.93 | 19.42 | 0 | Bedding | N74W/19SW |
| CZMW-10 | 100.33 | 204.61 | 18.41 | 0 | Bedding | N65W/18SW |
| CZMW-10 | 100.39 | 148.09 | 78.71 | 0 | Part. Open Fract | N58E/79SE |

# Planar Orientations

| Well ID | Depth (feet) | Dip Dir. (deg) | Dip (deg) | Aperture (mm) | Type | Strike/Dip (Quadrant) |
|---|---|---|---|---|---|---|
| CZMW-10 | 104.37 | 140.68 | 83.3 | 0 | Part. Open Fract | N51E/83SE |
| CZMW-10 | 104.73 | 143.55 | 86.52 | 0 | Filled Fracture | N54E/87SE |
| CZMW-10 | 104.75 | 142.48 | 80.32 | 0 | Part. Open Fract | N52E/80SE |
| CZMW-10 | 109.71 | 222.71 | 13.26 | 0 | Bedding | N47W/13SW |
| CZMW-10 | 111.23 | 217.3 | 11.93 | 0 | Bedding | N53W/12SW |